Model Selection and Parameters Estimation in Kinetic Thermal Evaluations Using Semiempirical Models

Roberto Sanchirico
Istituto di Ricerche sulla Combustione, CNR, P.le V. Tecchio, 80, 80125 Napoli, Italy

DOI 10.1002/aic.12711
Published online July 18, 2011 in Wiley Online Library (wileyonlinelibrary.com).

The minimum number of thermoanalytical experiments that should be considered with the aim of performing a complete and reliable kinetic analysis when using semiempirical models is the problem of concern. It is shown by means of a series of numerical experiments that three differential scanning calorimetric (DSC) dynamic runs performed at different heating rates provide a complete and reliable kinetic analysis while the topological structure of two DSC curves is enough to determine the semiempirical model (among reaction order and Sestack–Bergrenn) that better describe the experimental data. The procedure is analyzed by means of the simulation of a complex kinetic scheme and the results verified considering the thermal decomposition of cumene hydroperoxide. The proposed approach can be easily generalized to different kinetic models and is provided with a possible criterion devoted to identify autocatalytic processes by means of dynamical DSC experiments. © 2011 American Institute of Chemical Engineers *AIChE J,* 58: 1869–1879, 2012
Keywords: DSC, autocatalysis, parameters estimation, Matlab, cumene hydroperoxide

Introduction

Despite its enormous importance, the problem of gathering reliable thermokinetic information using nonisothermal techniques is still unresolved. The major part of the techniques is based on assumption of the so-called single step hypothesis.[1,2] This states that it is possible to write the reaction progress as the product of two independent terms, the first depending only on temperature and the second depending exclusively on the conversion degree.

$$\frac{d\alpha}{dt} = K(T)\, f(\alpha) \tag{1}$$

In dynamical differential scanning calorimetric (DSC) experiments, where the sample temperature is varied linearly and the specific heat power is measured, conversion degree is expressed as

$$\alpha = \frac{\int_0^t q(t)\, dt}{-\Delta H_{\mathrm{R}}} \tag{2}$$

where

$$-\Delta H_{\mathrm{R}} = \int_0^{\infty} q(t)\, dt = \frac{1}{\beta}\int_{T_{\mathrm{O}}}^{T_{\mathrm{end}}} q(T) dT \tag{3}$$

If one assumes the single step hypothesis, two approaches can be considered: the so-called model-free and the model-based techniques.[3–5] The first class of techniques includes all the methods that allow the determination of the dependence of the activation energy by the conversion. The second class of methods includes the strategies devoted to the determination of the best model that fit the experimental data. Each of these methods has their own peculiarities and limitations.[6–9] Despite huge literature on these topics, we have adopted here the approach reported by Militký and Sestak[10]: the problem that has to be faced is to find the vector of parameters $\underline{\vartheta} = [A\ E\ m\ a\ b\ c]'$ used for the kinetic constant of an Arrhenius type expression

$$K(T) = A\, T^m\ \exp\left(-\frac{E}{RT}\right) \tag{4}$$

and for $f(\alpha)$ the complete form of the Sestak–Berggren equation[11–13]

$$\mathrm{SB}(a,b,c): \quad f(\alpha) = \alpha^a (1-\alpha)^b [-\ln(1-\alpha)]^c \tag{5}$$

Equation 5 can be simplified, because it has been demonstrated that this form is redundant and the equation that should be adopted[14] is the form where $c = 0$

$$\mathrm{SB}(a,b): \quad f(\alpha) = \alpha^a (1-\alpha)^b \tag{6}$$

This is a well known equation that is adopted to model autocatalytic processes.[15] The dependence of the pre-exponential factor on temperature is generally neglected[10] setting $m = 0$ in Eq. 4.

The basic such model, other than SB(a,b), given in Eq. 6, is represented by the reaction order model RO(n) (Eq. 7)

$$\mathrm{RO}(n): \quad f(\alpha) = (1-\alpha)^n \tag{7}$$

The use of semiempirical models has also been proposed in the literature.[16] The application of these models is particularly

The author dedicates this work in memory of his father Mario.
Correspondence concerning this article should be addressed to R. Sanchirico at r.sanchirico@irc.cnr.it.

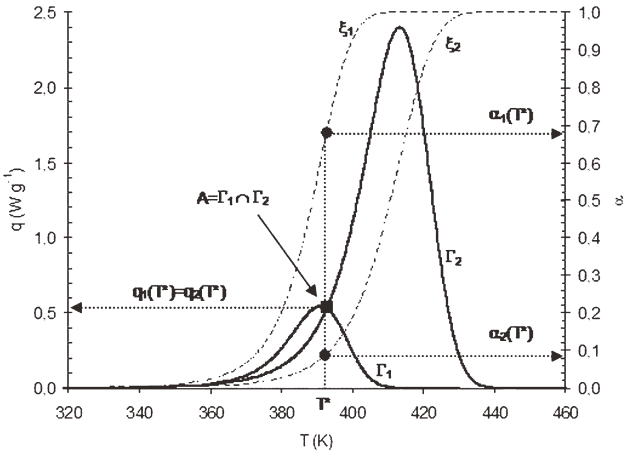

Figure 1. Heat powers (solid lines, Γ_i; $i = 1,2$; left scale) and conversions (dashed lines, ξ_i; $i = 1, 2$ right scale) at $\beta_1 < \beta_2$ (Case 1).

useful when either the detailed kinetic network is unknown or this knowledge is redundant. There are cases in which it is very difficult to gather reliable information on the whole reaction network involved in a given process. For example, this is the case of thermal decomposition processes in which hundreds of elemental steps are involved. This prevents the possibility of gathering valuable information on the thermokinetic characteristics of each elemental step in a "reasonable" time scale. In other cases, the knowledge of detailed elemental steps is redundant. For example, during the cure of a resin, often what is required is only the cure degree at a given temperature and reaction time without further details. Also, in this case, it is easily accomplished by means of use of semiempirical models.

A good kinetic analysis should assess the kinetic triplet [A, E, f(α)] suitable both to interpolate the current experimental data and predict the behavior of the system outside the actual initial conditions (extrapolation). For example, the last point is crucial in the context of a safety analysis.[15,17] The incorrect interpretation of the experimental data could lead to disastrous consequences if applied at industrial scale. When evaluating safety aspects concerned with reacting compounds (or mixtures), a large part of the problems could arise when an autocatalytic is confused with an *n*th-order process. In these circumstances, all the possible previsions gathered using this wrong prerequisite could lead to an underestimation of the safety parameters (adiabatic time to maximum rise, self-accelerating decomposition temperature (SADT), etc.) that could represent a root for severe industrial accidents.[18] Kinetic analyses require the choice of the analytical form of the model f(α) (model selection) and identify the value of the unknown parameters. It has been pointed out that a poor estimation of the kinetic model could lead to large errors also on Arrhenius parameters.[19]

Because of the complex nature of the objective function, usually the sum of the squared errors, the success of this approach is strongly affected by the proper choice of the initial values of the parameters. A strategy adopted to solve this problem involves the use of advanced numerical algorithms that attempt to find the global minimum.[20] The use of modern apparatus allows us to perform a large number of repeatable experiments, but the problem of determining the minimum number of runs that should be considered to gather reliable kinetic parameters is still unresolved. Thus, although a single dynamic run contains all the necessary information, more than one scan performed at different heating rates are required to identify the model correctly.[20–22]

A technique adopted to discriminate among different models is the Malek method.[23,24] This approach allows the model selection by analyzing the shape of the so-called $y(\alpha)$ and $z(\alpha)$ functions. These functions are built considering the data acquired performing different DSC scan at different heat rates. Although it is a powerful tool, this method could lead to wrong conclusions if activation energy is poorly estimated.[25]

In the successive sections, the following assumptions will be evaluated: a thermal event in a dynamical DSC run is represented by a single peak; single step approximation holds (Eq. 1 valid); the dependence of the rate constant is of an Arrhenius type with a constant pre-exponential factor and the reaction mechanisms do not change when varying the heat rate; the models considered are: SB(*a*,*b*) (Eq. 6) and RO(*n*) (Eq. 7).

Method Description

Let us consider two heat power vs. temperature curves Γ_1 and Γ_2 gathered in two dynamical DSC runs carried out starting at the same initial temperature $T_O = T(0)$ but at different heating rates $\beta_1 < \beta_2$

$$q_i(T) = K(T)\ f(\alpha_i)\ (-\Delta H_R), \quad i = 1,\ 2 \tag{8}$$

In the successive sections, the following circumstance will be evaluated:

Case 1: Γ_1 and Γ_2 intercept at a point $A = \Gamma_1 \cap \Gamma_2$ that is different from the origin (Figure 1): $\exists T^* > T_O$: $q_1\ (T^*) = q_2\ (T^*)$.

Case 2: Γ_1 and Γ_2 do not intercept (Figure 2), that is, $\forall T > T_O : q_1\ (T) < q_2\ (T)$.

In both the Cases 1 and 2 as $\forall T > T_O : \alpha_1\ (T) > \alpha_2\ (T)$ (or equivalently: $1 - \alpha_1\ (T) < 1 - \alpha_2\ (T)$, we have

$$\ln\left(\frac{\alpha_1}{\alpha_2}\right) > 0 \tag{9}$$

$$\ln\left(\frac{1-\alpha_1}{1-\alpha_2}\right) < 0 \tag{10}$$

The two inequalities 9 and 10 will be useful in the successive demonstrations. In the hypothesis of the Case 1, it will be

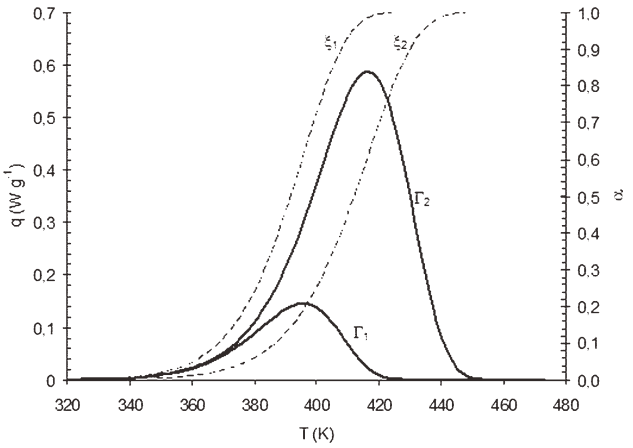

Figure 2. Heat powers (solid lines, Γ_i; $i = 1,2$; left side) and conversions (dashed lines, ξ_i; $i = 1,2$ right side) at heating rate $\beta_1 < \beta_2$ (Case 2).

demonstrated that RO(n) is not applicable; if SB(a,b) is applied, then $\frac{a}{b} > 0$ (more precisely: $0 < a < 1$ and $b > 0$).

In fact, in the case of existence of an intersection point different from the origin, if we consider the expression of $q = q(T)$ given in Eq. 8, at the intersection point: $q_1\ (T^*) = K\ (T^*)\ f\ (\alpha_1(T^*))\ (-\Delta H_R)$ and $q_2\ (T^*) = K(T^*)\ f(\alpha_2\ (T^*))\ (-\Delta H_R)$, dividing these two equations side by side, we get $q_1(T^*)/q_2(T^*) = \frac{K(T^*)\ f(\alpha_1(T^*))\ (-\Delta H_R)}{K(T^*)\ f(\alpha_2(T^*))\ (-\Delta H_R)}$ and after simplification $\frac{q_1(T^*)}{q_2(T^*)} = \frac{f(\alpha_1(T^*))}{f(\alpha_2(T^*))}$. As at the point A $= \Gamma_1 \cap \Gamma_2$: $q_1(T^*) = q_2(T^*)$, the previous equation reduces to $f(a_1(T^*)) = f(a_2(T^*))$, that is

$$\frac{f(\alpha_1(T^*))}{f(\alpha_2(T^*))} = 1 \tag{11}$$

Now, if we consider RO(n), Eq. 11 is $(1 - \alpha_1^*/1 - \alpha_2^*)^n = 1$; as $n > 0$, this last equation is verified if and only if $\alpha_1(T^*) = \alpha_2\ (T^*)$ against the fact that $\alpha_1\ (T^*) > \alpha_2\ (T^*)$ (which is absurd).

If we consider the SB(a,b) model, in this case, Eq. 11 is $(\alpha_1^*/\alpha_2^*)^a(1 - \alpha_2^*/1 - \alpha_1^*)^b = 1$; taking the logarithm of both sides of the last relation, we get $a\ln(\alpha_1^*/\alpha_2^*) + b\ln(1 - \alpha_1^*/1 - \alpha_2^*) = 0$, that is, considering the inequalities 9 and 10 $\frac{a}{b} = -\ln(\frac{1-\alpha_1^*}{1-\alpha_2^*})/\ln(\frac{\alpha_1^*}{\alpha_2^*}) > 0$. This inequality is satisfied either for $a < 0$ and $b < 0$ or $a > 0$ and $b > 0$. The first possibility has to be ruled out because it has been demonstrated[26] that $0 < a < 1$. Thus, if SB(a,b) is applicable, we should expect $0 < a < 1$ and $b > 0$.

In this hypothesis of Case 2, that is, in the case that the two heat power curves do not intercept in a point different from the origin; if RO(n) applies, $n > 0$, then SB(a,b) does not apply.

In this case, $\forall\ T > T_O : q_1\ (T) < q_2\ (T)$ dividing Eq. 8 side by side written for $i = 1$ and $i = 2$ and taking the logarithm of both side of the resulting expression, the following inequality holds

$$\ln\left(\frac{q_1(T)}{q_2(T)}\right) = \ln\left(\frac{f(\alpha_1(T))}{f(\alpha_2(T))}\right) < 0 \tag{12}$$

Let us consider RO(n). Considering Eq. 12 and recalling Eq. 10, we get $\ln(q_1/q_2) = n\ln(1 - \alpha_1/1 - \alpha_2) < 0$, the last inequality being satisfied only if $n > 0$.

If we consider the Sestack–Bergrenn (SB) model, the relation 12 written for this case is $\ln(q_1/q_2) = a\ln(\frac{\alpha_1}{\alpha_2}) + b\ \ln(\frac{1-\alpha_1}{1-\alpha_2}) < 0$. Considering Eq. 9, it follows that $a < -\ b\ln(\frac{1-\alpha_1}{1-\alpha_2})/\ln(\frac{\alpha_1}{\alpha_2})$ but as $\forall T > T_O$: $-\ \ln(\frac{1-\alpha_1}{1-\alpha_2})/\ln(\frac{\alpha_1}{\alpha_2}) > 0$ the last inequality is not verified when $a > 0$ and $b < 0$, which holds in the following cases: (1) $a > 0$ and $b > 0$, (2) $a < 0$ and $b < 0$, and (3) $a < 0$ and $b > 0$; $\frac{a}{b} > 0$ holds in Case 1; hence, (1) has to be ruled out; (2) and (3) are not allowed because a has to be $0 < a < 1$.

Model selection and initial estimation of the parameters

It will be shown that for the determination of the kinetic triplet, [A, E, f(α)] are sufficient three dynamical runs carried out at different heating rates, while for the determination of the kinetic model alone two runs are enough.

Let us consider two dynamical runs carried out in dynamical conditions starting from the same initial temperature T_O and at two different heating rate $\beta_1 < \beta_2$. Writing Eq. 8 for each heating rate and dividing the resulting equations side by side, we get

$$\frac{q_1(T)}{q_2(T)} = \frac{f(\alpha_1(T))}{f(\alpha_2(T))} \tag{13}$$

The last equation holds both in the Cases 1 and 2. Let us consider SB(a,b). Substituting this model in Eq. 13 and taking the logarithms of both side of the resulting equation, we get $\ln(q_1/q_2) = a\ln(\frac{\alpha_1}{\alpha_2}) + b\ \ln(1 - \alpha_1/1 - \alpha_2)$.

Dividing side by side by $\ln(\frac{\alpha_1}{\alpha_2})$ (or by $\ln(1 - \alpha_1/1 - \alpha_2)$ gathering an analogue relation), we get

$$\frac{\ln\left(\frac{q_1}{q_2}\right)}{\ln(\frac{\alpha_1}{\alpha_2})} = a + b\ \frac{\ln\left(\frac{1-\alpha_1}{1-\alpha_2}\right)}{\ln\left(\frac{\alpha_1}{\alpha_2}\right)}$$

Thus, if we introduce the following variables $y = \ln(\frac{q_1}{q_2})/\ln(\frac{\alpha_1}{\alpha_2})$ and $x = \ln(\frac{1-\alpha_1}{1-\alpha_2})/\ln(\frac{\alpha_1}{\alpha_2})$, it follows that if the SB(a,b) is the correct model, the points y vs. x should align; the slope of this line is b, while the intercept is a

$$y = a + b\,x \tag{14}$$

Moreover, in the circumstances considered in the Case 1, we should gather $0 < a < 1$ and $b > 0$.

Furthermore, in the hypothesis of the Case 2, if RO(n) holds by applying Eq. 14, we should get an intercept $a = 0$ and a slope $b = n > 0$. Obviously, this result could also be derived by plotting $\ln(\frac{q_1}{q_2})$ vs. $\ln(\frac{1-\alpha_1}{1-\alpha_2})$; if the linear regression of these points gives an intercept zero, the slope is the reaction order n.

Once the model f(α) is estimated, its derivative f′(α) can be used for the estimation of the activation energy and of the pre-exponential factor. For this purpose, the extended Kissinger's method[27,28] could be used. This require at least three experimental curves gathered in different dynamical runs carried out using different heating rate $\beta_1 < \beta_2 < \beta_3$

$$\ln\left(\frac{\beta_i}{T_{i,\max}}\right) = -\frac{E}{\mathrm{R}\ \mathrm{T}_{i,\max}} + \ln\left(\frac{\mathrm{AR}}{E}\phi_O(\alpha_{i,\max})\right)\ \ (i = 1, 2, 3) \tag{15}$$

where, $\phi_O\ (\alpha_{i,\max}) = -\dot{f}(\alpha_{i,\max})$. Using Eq. 15, from the plot $\ln(\frac{\beta_i}{T_{i,\max}})$ vs. $\frac{1}{T_{i,\max}}$, it is possible to determine E from the slope and A from intercept of this line.

The aim of the third run, at this point, is twofold. It can also be used to verify the results gathered about the model using the first two runs. In fact, the method described above can be applied considering other than (Γ_1, Γ_2) also the pairs (Γ_2, Γ_3), (Γ_1, Γ_3), and the corresponding integral curves (in Figure 3, $A = \Gamma_1 \cap \Gamma_2$; $B = \Gamma_2 \cap \Gamma_3$; $C = \Gamma_1 \cap \Gamma_3$).

In this case, the meaning of the variables x, y in Eq. 14 has to be adapted accordingly. If we consider three heating power curves $q_i = q(\beta_i,T)$ (and the correspondent conversion curve $\alpha_i = \alpha(\beta_i,T)$) with $i = 1, 2, 3$, if we set

$$x_{i,j} = \frac{\ln\left(\frac{1-\alpha_i}{1-\alpha_j}\right)}{\ln\left(\frac{\alpha_i}{\alpha_j}\right)} \tag{16a}$$

$$y_{i,j} = \frac{\ln\left(\frac{q_i}{q_j}\right)}{\ln\left(\frac{\alpha_i}{\alpha_j}\right)} \tag{16b}$$

with $(i,j) = (1,2), (2,3), (1,3)$, Eq. 14 can be written considering the pair (i,j) and setting each time $x = x_{i,j}$ and $y = y_{i,j}$ (Eqs. 16a and 16b). It is evident that we should observe

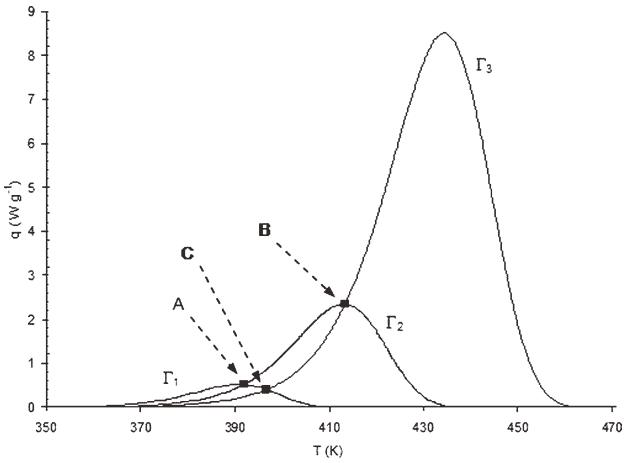

Figure 3. Basic set of curves necessary to perform a whole kinetic analysis.

Heat powers refer to three DSC dynamical runs carried out at constant heating rate $\beta_1 < \beta_2 < \beta_3$. Γ_1, Γ_2, Γ_3 refer to β_1, β_2, β_3, respectively. $A = \Gamma_1 \cap \Gamma_2$, $B = \Gamma_2 \cap \Gamma_3$, $C = \Gamma_1 \cap \Gamma_3$.

similar results considering all the different combinations of indexes.

The values of the Arrhenius and kinetic model parameters assessed previously were adopted as initial estimate in a successive optimization procedure. As it will be shown in the next section, multivariate ordinary least square could be applied for the search of the minimum over the parameter space of the sum of the squared errors built considering all the data collected at the different heating rates.

Last but not the least, it should be pointed out that the procedure described considering the RO(n) and SB(a,b) model can be easily generalized also by considering different kinetic models. Given a kinetic model f(α), the basic idea is to apply Eq. 13 and introduce suitable variables that lead to mathematical correlations that allow us the assessment of the desired parameters. For example, if we consider the well-known Johnson–Mehl–Avramy [JMA(v)] model[16]

$$\mathrm{JMA}(v): \quad f(\alpha) = v\,(1-\alpha)\,[-\ln(1-\alpha)]^{1-\frac{1}{v}}$$

a way that could lead to the initial estimation of the parameter v is the following: Eq. 13 in logarithmic form written in the case of the JMA(v) model for two heating rate β_1, β_2 is $\ln(\frac{q_1}{q_2}) = \ln(\frac{1-\alpha_1}{1-\alpha_2}) + (1-\frac{1}{v})\ln(\ln(1-\alpha_1)/\ln(1-\alpha_2))$; dividing each side of the last equation by $\ln(\frac{1-\alpha_1}{1-\alpha_2})$ we get $\frac{\ln(\frac{q_1}{q_2})}{\ln(\frac{1-\alpha_1}{1-\alpha_2})} = 1 + (1-\frac{1}{v})\ln(\frac{\ln(1-\alpha_1)}{\ln(1-\alpha_2)})/\ln(\frac{1-\alpha_1}{1-\alpha_2})$. Thus, if the experimental points $w = \ln(\frac{q_1}{q_2})/\ln(\frac{1-\alpha_1}{1-\alpha_2})$ vs. $z = \ln(\frac{\ln(1-\alpha_1)}{\ln(1-\alpha_2)})/\ln(\frac{1-\alpha_1}{1-\alpha_2})$ align with intercept equal to one, the slope is equal to $(1-\frac{1}{v})$

$$w = 1 + \left(1 - \frac{1}{v}\right) z \tag{16c}$$

Also in this case, when more runs are available, Eq. 13 can be adapted accordingly to the different combination of indexes.

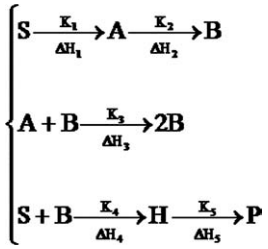

Scheme 1. Reaction network adopted to carry out the numerical experiments.

Example of Application

Numerical experiments

With the aim at validating the method described in the previous section and show the whole optimization procedure, a series of numerical experiments have been performed considering the reaction network reported in the Scheme 1.

This scheme is composed of different elemental steps and involve (Step 2 and 3) an autocatalytic subprocess.

For this reaction network, the material balance equations reported in Eq. 17 can be written as follows

$$\begin{cases} \dfrac{dC_S}{dt} = -k_1 C_S - k_4 C_S C_B \\ \dfrac{dC_A}{dt} = k_1 C_S - k_3 C_A C_B - k_2 C_A \\ \dfrac{dC_B}{dt} = k_2 C_A - k_4 C_S C_B + k_3 C_A C_B \\ \dfrac{dC_H}{dt} = k_4 C_B C_S - k_5 C_H \\ \dfrac{dC_P}{dt} = k_5 C_H \end{cases} \tag{17}$$

The process has been supposed to be taking place in an homogenous phase.

The heat effects associated to each step are

$$\begin{cases} \varphi_1 = V\ k_1 C_S\ (-\Delta H_1) \\ \varphi_2 = V\ k_2 C_A\ (-\Delta H_2) \\ \varphi_3 = V\ k_3 C_A C_B\ (-\Delta H_3) \\ \varphi_4 = V\ k_4 C_B C_S\ (-\Delta H_4) \\ \varphi_5 = V\ k_5 C_H\ (-\Delta H_5) \end{cases} \tag{18}$$

Thus, the whole specific heat power is

$$q = \frac{1}{M_O} \sum_{i=1}^{5} \varphi_i \tag{19}$$

All the calculations were performed using the software Matlab.[29] The integration of Eq. 17 was carried out considering the thermokinetic parameters reported in Table 1.

In all cases, $M_O = 0.0050$ g, $V = 5 \times 10^{-6}$ dm^3 and the following initial conditions $C_{S,0} = 5$ mol (dm^3)$^{-1}$, $C_{A,0} = C_{B,0} = C_{H,0} = C_{P,0} = 0$ mol (dm^3)$^{-1}$ were considered. The linear heating temperature profiles were obtained starting

Table 1. Thermokinetic Parameters Used for the Elemental Steps in the Reaction Network of Scheme 1

Steps	A_i (s^{-1})	E_i (J mol^{-1})	$-\Delta H_i$ (J mol^{-1})
1	1.67E+09	92,092	62,790
2	1.67E+10	96,278	87,906
3	1.67E+09	75,348	79,534
4	1.67E+10	83,720	54,418
5	1.67E+08	79,534	83,720

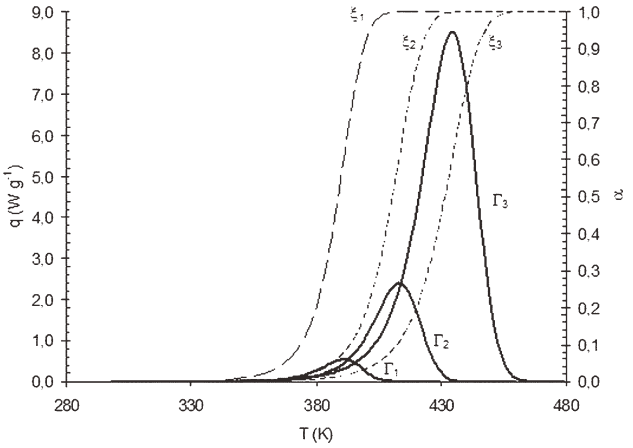

Figure 4. Heat powers ("Clean data") (Γ_i, i = 1, ... 3; solid lines, left axis) and corresponding conversions (ξ_i, i = 1, ...3; dashed lines, right axis) evaluated at different heating rates (β_1 = 1 , β_2 = 5 and β_3 = 20 K min^{-1}).

from the same initial temperature $T_O = 298.16$ K and using the following heat rates $\beta_1 = 1$, $\beta_2 = 5$, and $\beta_3 = 20$ K min^{-1} (we will refer to these data as the "True Data"). With the aim of mimicking a real data set and to perform the consequent necessary calculations, to the specific heat power gathered at β_i: $q_i = q_i(t, \beta_i)$ (i = 1, 2, 3) was added a random Gaussian noise $\varepsilon = N(\mu, \sigma^2)$ with mean $\mu = 0$ and variance $\sigma^2 = 3.3 \times 10^{-9}$ (we will refer to these data sets as the "Raw Data": $q_{i,Raw} = q_i(t, \beta_i) + \varepsilon$). The numerical data thus obtained were filtered using a Savitzky–Golay filter (Matlab command[29]: smooth with "sgolay" parameter with span = 51 and order = 4) and after sampling at each heating rate of about 200 points,[30] the resulting set of data were used in the successive calculations (we will refer to these data as the "Clean Data").

In Figure 4 are reported the specific heat powers (left axis) and the corresponding conversion curves (right axis) gathered at the different heat rates. Heat powers were calculated using Eq. 19, while conversions were calculated using Eq. 2. For the integration of the system of Eq. 17, we used simulink [integration method[29]: ODE 15s (Stiff/NDF)].

The mean value for the heat of reaction (calculated considering the "clean" specific heat power and using Eq. 3 resulted $\Delta H_R = -714.8$ J g^{-1}. It should be stressed that the use of semiempirical models could be considered as a possible way to lump in an apparent kinetic scheme, the complex nature of the real process under study.

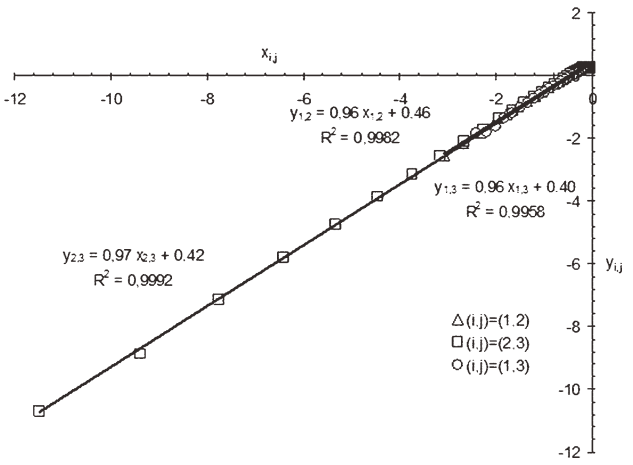

Figure 5. Application of Eq. 14 considering SB(a,b) model for the couples of curves at β_1 = 1 and β_2 = 5 K min^{-1} [points (i,j) = (1,2)] at β_2 = 5 and β_3 = 20 K min^{-1} [points (i,j) = (2,3)] and at β_1 = 1 and β_3 = 20 K min^{-1} [points (i,j) = (1,3)].

Preliminary assessments

The analysis of Figure 4 immediately leads to ruling out the RO(n) model because of the presence of three different intersection points. The remaining possibility is SB(a,b) with $0 < a < 1$ and $b > 0$. If SB(a,b) holds the variables (x,y) in Eq. 14, it should align with slope equal to a and intercept b. In Figure 5 are reported the plots $y_{i,j}$ vs. $x_{i,j}$ (Eq. 14, 16a, and 16b), and in Table 2, the values of the SB exponents for the different combination of indexes.

It should be pointed out that the temperature ranges for the above calculations should exclude the "tails" of the curves at β_i,β_j (evaluation temperature range in Table 2). In fact, due to the nonlinear transformations involved, the experimental errors could amplify when two curves are too close, thus leading to possible inconsistent results.

Kissinger's method was applied considering Eq. 15. The linear interpolation of $\ln(\frac{\beta}{T_{max}^2})$ vs. $\frac{1}{T_{max}}$ allowed (T_{max} were found at 391.4, 413.0, and 435 K at β = 1.0, 5.0, and 20 K min^{-1}, respectively) the determination of an activation energy of $E_O = 90{,}668$ J mol^{-1} and a pre-exponential factor $A_O = 2.61\ 10^9$ s^{-1}. As the calculation of the pre-exponential factor require the derivative of the kinetic model, that is, in the case of SB(a,b) is $f'(\alpha) = a\alpha^{a-1}(1-\alpha)^b - b\alpha(1-\alpha)^{b-1}$, for a and b were used the mean values $a_O = 0.43$ and $b_O = 0.96$ reported in Table 2.

Kinetic triplet assessment

The values of a_O, b_O, A_O, and E_O assessed previously were used as initial estimate of the kinetic parameters for the kinetic model f(α) and the Arrhenius parameters A and E. The final estimate of the thermokinetic parameters was assessed by means of the minimization of the sum of the squared errors (Matlab command: *lsqnonlin*[29]: this routine solve the minimization problem either using the "trust-region-reflective" (default) or "Levenberg–Marquardt" method) calculated considering all the data at the different heating rates,[31] that is, it minimized the following objective function[32]

$$\Psi(\underline{\vartheta}) = \sum_{i=1}^{3}\sum_{j=1}^{N_i}\left[q(\beta_i, t_{i,j}) - g(\underline{\vartheta}, t_{i,j})\right]^2 \text{over the parameter space } \underline{\hat{\vartheta}} = \min_{\underline{\vartheta}} \Psi(\underline{\vartheta})$$

Table 2. Calculated Values for the Exponents of the SB(a,b) Model Using Eq. 14 Along with the Corresponding Evaluation Temperature Range

Data Set At	Evaluation Temperature Range (K)	a	b
β_1, β_2	380–405	0.46	0.96
β_2, β_3	390–435	0.42	0.97
β_1, β_3	385–410	0.40	0.96
Mean value		0.43	0.96

Table 3. Final Estimate of the Arrhenius and SB(*a*,*b*) Model Parameters Along with Their 95% Confidence Intervals

Parameter	Mean Value	95%, Left Error Bound	95%, Right Error Bound
$\hat{A}$ (s^{-1})	2.69E+09	2.14E+09	3.24E+09
$\hat{E}$ (J mol^{-1})	90,605	89,867	91,343
$\hat{a}$	0.42	0.41	0.43
$\hat{b}$	0.95	0.94	0.96

with $g(\underline{\vartheta}, t) = \frac{d\alpha}{dt}\left(-\Delta H_{R,m}\right)$ and α the solution of the differential equation $\frac{d\alpha}{dt} = K(T)f(\alpha)$ (with $T = T_0 + \beta_i t$); the last differential equation was integrated setting an initial value of the conversion $\alpha_0 = 10^{-3}$ and considering [on the (α,t) curves (clean data)] the corresponding time $t_{0,i}$. That is, this differential equation was integrated, at each heating rate β_i, considering the following initial conditions $\alpha\ (\beta_i, t_{O,i}) = \alpha_0 = 10^{-3}\ \forall\ i = 1\ldots3$.

Because of the extreme stiffness of the optimization of the Arrhenius parameters A and E, a reparametrized expression of the kinetic constant was used.[33–35] By means of a suitable centering and scaling procedure of the Arrhenius parameters their multicollinearity is greatly reduced

$$K(T) = \exp\left[r - d\frac{E_0}{R}\left(\frac{1}{T} - \frac{1}{T_{\mathrm{Ref}}}\right)\right] \tag{20}$$

where T_{Ref} is a reference temperature calculated as the mean value between the temperature at the first inflection point of the peak at lowest heating rate β_1 and the temperature at the second inflection point at the highest heat rate β_3 (in this case, resulted $T_{\mathrm{Ref}} = 412.5$ K). With this assumption, the new parameters that have to be identified are $\underline{\vartheta'} = [r, d, a, b]^T$. The initial estimate $\underline{\vartheta'_0} = [r_0, d_0, a_0, b_0]^T$ is calculated starting from the original parameters A_0, E_0, setting $d_0 = 1$ and deriving r_0 by means of the following transformation

$$r_0 = \ln(A_0) - \left(\frac{E_0\ d_0}{R\ \ T_{\mathrm{Ref}}}\right) \tag{21}$$

It has to be observed that r_0 strongly depends on the values of A_0 and E_0. This choice along with $d_0 = 1$ lead to the determination of an Hessian matrix H ($\mathrm{H} = (h_{i,j}) : h_{i,j} = \frac{\partial^2 \Psi}{\partial\vartheta_i \partial\vartheta_j}$) that show at the minimum $\vartheta = \underline{\hat{\vartheta}}$ the minimum value of the so called spread number defined as $N\ (H) = \ln(\lambda_{\max}) - \ln\ (\lambda_{\min})$ ($\lambda_{\min}$ and $\lambda_{\max}$ are the maximum and minimum eigen value of H, respectively).

The initial values of the centered and scaled Arrhenius parameters along with the initial estimate of the exponents of the SB model adopted in the successive optimization procedure resulted to be $r_{\mathrm{O}} = -4.74$, $d_{\mathrm{O}} = 1.00$, $a_{\mathrm{O}} = 0.43$, and $b_{\mathrm{O}} = 0.96$. After the optimization performed considering these initial values, the corresponding parameters were determined by means of the following inverse transformations

$$\hat{E} = \hat{d}\ E_0 \tag{22}$$

$$\hat{A} = \exp\left(\hat{r} + \frac{E_0\ \hat{d}}{R\ \ T_{\mathrm{Ref}}}\right) \tag{23}$$

and the set of parameters $\underline{\hat{\vartheta}} = [\hat{A},\ \hat{E},\ \hat{a},\ \hat{b}\ ]^T$ was assessed.

For gathering inferential information about the identified parameters, these were reoptimized by removing their centering and scaling, that is, starting from these final estimates and using for $K(T)$ of the expression 4 (with $m = 0$). This procedure allowed (Matlab command: *nlparci*[29]) the calculation of the 95% confidence intervals for the estimated parameters. These results are reported in Table 3, while in Figure 6 are reported the calculated conversion curves and the corresponding pseudoexperimental (clean) data.

Experimental and Numerical Verifications

Experimental verification

To the aim at showing the application of the method discussed above, three DSC runs carried out on cumene hydroperoxide (CHP) were considered. This compound is an important industrial intermediate for which different kinetic studies on its thermal decomposition process have been proposed.[36–41] A literature survey pointed out that the major discrepancy among the available information is concerned with the kinetic nature of this thermal decomposition process. In fact, they are reported both different *n*th-order[39,40] and autocatalytic kinetics.[37,38,41]

Although during the past years, a huge effort has been paid toward the detailed understanding of the kinetic mechanisms involved during the thermal decomposition of CHP, to date is available a considerable but not exhaustive knowledge on the whole kinetic network involved. Reaction Schemes 2, 3, and 4 highlight some mechanistic information published on the topic.[38] These schemes explain, by means of radical mechanisms, the presence among the thermal decomposition products of acetophenone and carbinol (Scheme 2), dicumylperoxide (Scheme 3), and α-methylstirene (Scheme 4).

Nevertheless, these schemes represent only a partial view of the real reaction network. For example, it should be stressed that although this thermal decomposition process is reported to be as autocatalytic, in our knowledge the autocatalytic agent has not yet been assessed. This prevents the assessment of a complete set of material balance equations that takes in to account of all the possible elemental steps involved. Thus, one possible way to approach a realistic kinetic analysis could be based on the use of semiempirical models.

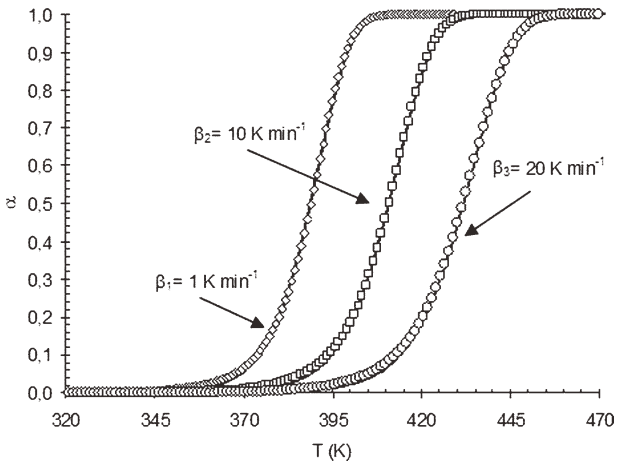

Figure 6. Calculated (solid line) and pseudo-experimental (Clean data, symbols) conversions at β_1 = 1 K min^{-1}, β_2 = 5 K min^{-1}, and β_3 = 20 K min^{-1}.

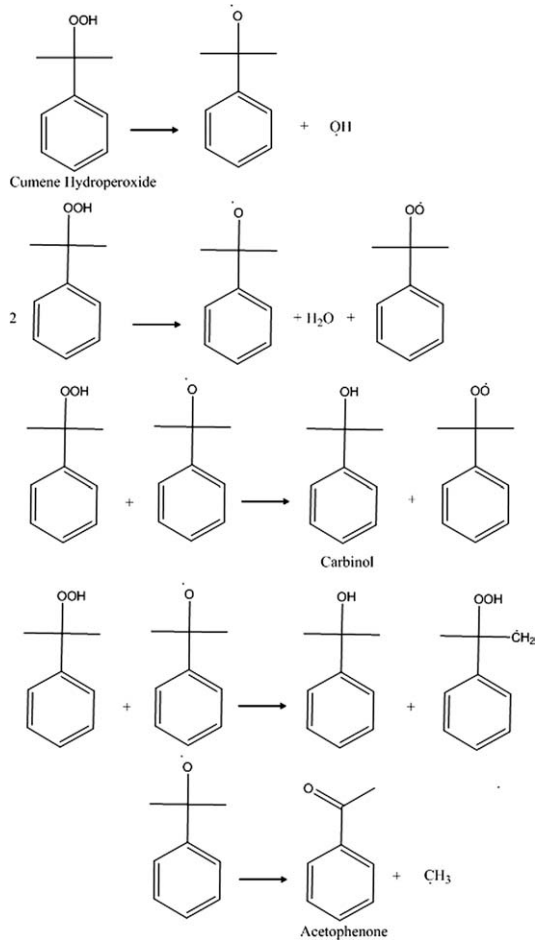

Scheme 2. Kinetic scheme that explain the presence of carbinol and acetophenone among the thermal decomposition product of CHP.

Materials and method

CHP (80 w/w % in Cumene) was purchased by Sigma Aldrich. DSC runs were performed using a PerkinElmer DSC 8000 calorimeter equipped with an Intracooler II cooling system. Baseline calibration was performed over 273–673 K temperature range. As calibration standard indium was used (expected temperature and fusion heat are equal to 429.76 K and 28.45 J g^{-1}, respectively). Dynamic runs were carried out

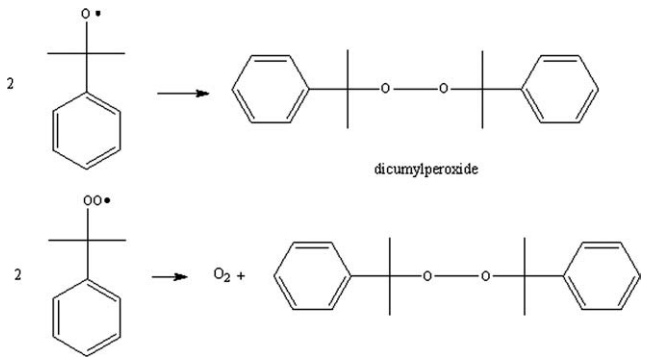

Scheme 3. Kinetic scheme that explain the presence of dicumylperoxide among the thermal decomposition product of CHP.

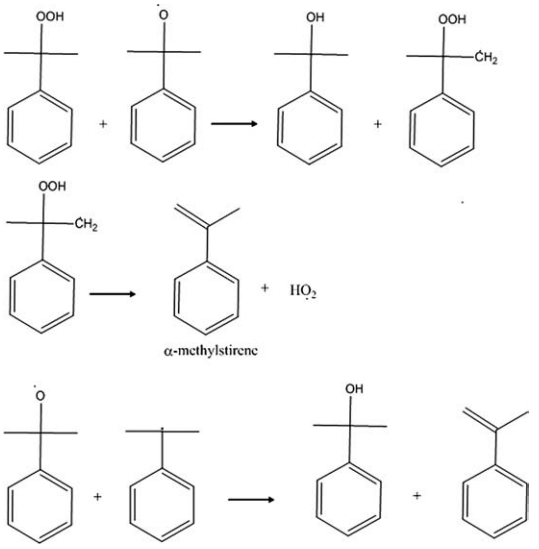

Scheme 4. Kinetic scheme that explain the presence of α-methylstirene among the thermal decomposition product of CHP.

on samples of approximately 2 mg using high pressure capsules (PerkinElmer part n. B018 2901 capable to withstand up to 100 bar of internal pressure) and adopting temperature ramps started at 323 K with heating rates of 1.5, 10, and 20 K min^{-1}. Isothermal DSC experiments were performed at 428, 433, and 443 K using the same capsules adopted for the dynamic experiments with samples of 2.4–2.8 mg.

Results and discussion

Dynamic DSC Runs: Parameters Identification. In Figure 7, it is shown the original signal collected during a run performed on a sample of CHP at 10 K min^{-1} along with the corresponding baseline, the consequent subtracted peak and the conversion curve. In all cases, baselines were determined using the tangential area-proportional method.[42] In Table 4, the principal characteristic of the DSC peaks along with the experimental conditions adopted are reported.

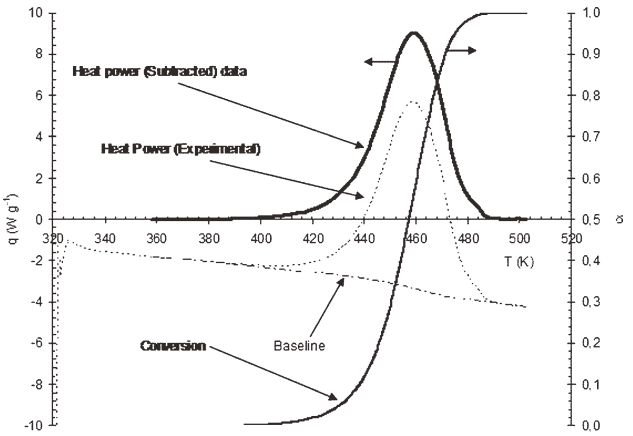

Figure 7. Experimental, tangential area-proportional baseline, and subtracted peak (left scale) along with its corresponding conversion curve (right scale) in a dynamic DSC run carried out on CHP at β = 10 K min^{-1}.

Table 4. Experimental Conditions Adopted and Principal Results Obtained During the DSC Dynamic Runs Carried Out on CHP

Sample Mass (mg)	β (K min^{-1})	T_{max} (K)	$-\Delta H_R$ (J g^{-1})
2.2	1.5	430	1692
2.1	10.0	459	1638
2.2	20.0	473	1613

The heat of decomposition considered for the successive calculations was the mean of the values reported in Table 4 ($-\Delta H_R = 1648 \pm 41$ J g^{-1}). Equation 14 was applied to all the possible couples of curves allowing the determination of an estimate of the kinetic exponents a and b reported in Table 5.

The mean values of the kinetic exponents $a_O = 0.44$ and $b_O = 0.95$ were used when applying Eq. 15. The application of the extended Kissinger's method allowed an estimation of the pre-exponential factor of $A_O = 1.31E+09$ s^{-1} and of an activation energy of $E_O = 95{,}895$ J mol^{-1}. These values were adopted to determine the following values of the scaled and centered parameters $r_O = -4.41$, $d_O = 1.00$, $a_O = 0.44$, and $b_O = 0.95$, which have been used as initial estimate for the successive identification procedure. Assuming a reference temperature of $T_{Ref} = 454$ K and setting the initial conversion degree at $\alpha_0 = 10^{-3}$, the application of the procedure described above led to the assessment of the final estimates reported in Table 6.

In Figure 8 both the experimental and the calculated curves are reported. The analysis of these results points out a good agreement among experimental data and theoretical evaluations and confirms the autocatalytic nature of the thermal decomposition of CHP.

Isothermal DSC Runs: Extrapolations. For the purpose to shown that the parameters identified using the methods described in the previous paragraphs can be used for extrapolations too as a real world application, a series of isothermal DSC runs were performed on CHP heating the sample starting in all cases from an initial temperature of 323 K up to the desired isothermal temperatures with an heating rate of 20 K min^{-1}. With the aim at acquiring the corresponding experimental baselines, after the isothermal runs the reacted samples were quenched at ambient temperature and resubmitted to the same thermal history. These baselines were subtracted to the first signal and the subtracted curves were used for the successive verification. In Figure 9, the signal, the baseline, and the corresponding subtracted signal (left scale) along with the temperature history (sample temperature, right scale) for the run carried out on CHP at 428 K are reported.

It should be observed that the shape of the specific heat power curve reported in Figure 9 confirms the autocatalytic nature of the thermal decomposition of CHP (due to the autocatalysis, this curve present an initial acceleratory phase, at the contrary of an nth-order process in which these curves show a strictly decreasing behavior).

Table 5. Calculated Values for the Exponents of the SB(a,b) Model Using Eq. 14 in the Case of the Thermal Decomposition of CHP

Data Set At	Evaluation Temperature Range (K)	a	b
β_1, β_2	405–450	0.40	0.89
β_2, β_3	425–480	0.52	1.09
β_1, β_3	410–450	0.40	0.88
Mean value		0.44	0.95

Table 6. Final Estimate of the Arrhenius and SB(a,b) Model Parameters Along with Their 95% Confidence Intervals in the Case of the Thermal Decomposition of CHP

Parameters	Mean Value	95%, Left Error Bound	95%, Right Error Bound
$\hat{A}$ (s^{-1})	3.728E+08	3.726E+08	3.729E+08
$\hat{E}$ (J mol^{-1})	91,220	91,101	91,338
$\hat{a}$	0.45	0.43	0.46
$\hat{b}$	0.93	0.90	0.96

The controlled thermal histories used to heat the samples at the desired temperatures allowed (instead of using arbitrary values for this important parameter) the determination of the initial value of the conversions degree at the beginning of the different isothermal phases.

The readings on the correspondent experimental conversion vs. temperature curve gathered in dynamical condition (initial temperature 323 K heating rate $\beta = 20$ K min^{-1}; Figure 8) allowed the determination of the following values of the initial conversion degrees: $\alpha_O = 0.013$, 0.021, and 0.053 at the temperatures adopted for the isothermal experiments (428, 433, and 443 K, respectively). These values were used to integrate the mass balance Eq. 1 at the different temperatures using the SB model and the values of parameters reported in Table 6. The results concerned with these runs are reported in Figure 10 and clearly show a good agreement between the experimental data and the calculated (extrapolated) curves.

Numerical verification

The minimum of the objective function (sum of squared errors) that it is possible to find using the method of the least squares depends on the choice of the initial values of the parameters: poorly estimated initial values could lead to a local minimum with correspondent wrong parameters estimates. To the aim at showing that the minimum of the objective function found by means of the procedures discussed above is the absolute minimum of this function, a global optimization procedure has been carried out both for the numerical experiments and the real data concerned with the thermal decomposition of CHP.

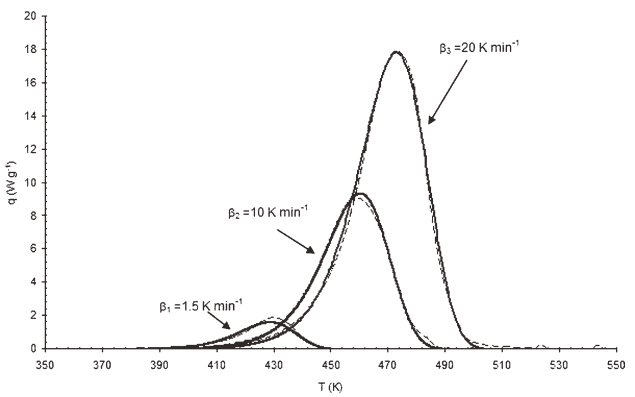

Figure 8. Experimental DSC (dashed) and calculated (solid) curves at $\beta = 1.5$, 10, and 20 K min^{-1} (heat rate is reported on the graph near the respective curve) collected in the case of the thermal decomposition of CHP.

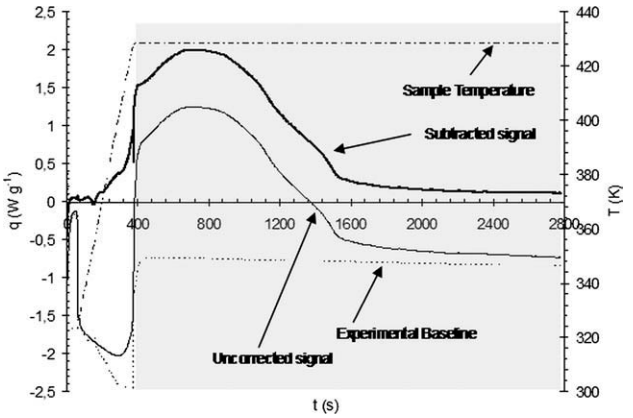

Figure 9. Uncorrected signal, experimental baseline, subtracted signal (left Scale), and Temperature program (right Scale) acquired during the isothermal run carried out on CHP at T_{Iso} = 428 K.

The grey area highlight the zone used for the calculation of the isothermal conversions.

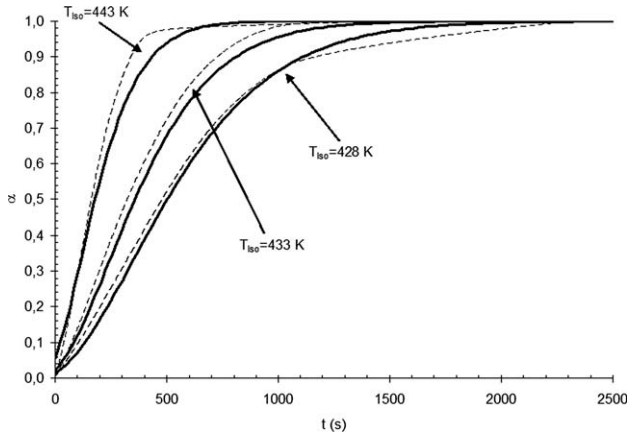

Figure 10. Experimental DSC isothermal conversions (dashed) and calculated extrapolation (solid) curves at T_{Iso} = 428, 433, and 443 K (heating phase started at T_O = 323 K with an heating rate β = 20 K min^{-1}) concerned with the thermal decomposition of CHP.

Absolute minima were determined using Tomlab software[43] and in particular the glbsolve routine.[44] The global optimization routine glbSolve is an implementation of the DIRECT algorithm,[45] which is a modification of the standard Lipschitzian approach that eliminates the need to specify a Lipschitz constant.

This algorithm runs a predefined number of iterations and considers the best function value found as the optimal one. The results of these verifications are reported in Table 7 both for the numerical (Figure 4) and for the DSC experiments carried out on CHP (Figure 8).

The program was run adopting 50 iterations and choosing for the lower and upper bounds of the variables the values reported in the first and second column of Table 7. It should be noted that these values allow to explore a very huge hypercube in the space of the original parameters [for example, assuming A_O = 1.31E+09 s^{-1} and E_O = 95,895 J mol^{-1}, the values estimated using the Kissinger's method in the case of the thermal decomposition of CHP and calculating by means of Eqs. 22 and 23, the corresponding values of the parameters, pre-exponential factor is varying in the range A = [0–4.75 × 10^{+15}], activation energy in the range E = [0–143,842]. a = [0–1] is varying over all the possible admissible values, the exponent b has to be greater than zero and usually is not grater than 2 thus b = [0–3] surely contain the true value of this parameter. A similar situation can be verified also considering the case of the numerical experiments (simulation of Scheme 1)]. Also, in this case, the numerical values of the parameters determined using glbSolve (Global Minimum) were adopted as an initial estimate in a successive optimization procedure performed using *lsqnonlin*[29] (final estimate in Table 7).

The data summarized in Table 7 allow us to calculate the corresponding values of the Arrhenius and kinetic model parameters that result equal to those found in the previous sections applying the proposed method (Tables 3 and 6). This means that in both the cases of numerical experiments and thermal decomposition of CHP, it is possible to determine the same absolute minima either using the proposed method or applying a global optimization procedure.

Conclusions

It has been shown that when using semiempirical models [RO(n), SB(a,b)], two curves are enough to determine the kinetic model that best describe the experimental data, while three curves are sufficient to asses the kinetic triplet. The new approach is not devoted to replace the existing kinetic evaluation methods but should be considered as a supplementary tool for kinetic evaluations.

The simple fact that two curves intercept in a point different from the origin allows us to conclude that RO(n) has to be ruled out and the application of SB(a,b) should provide $0 < a < 1$ and $b > 0$. This last circumstance highlights the autocatalytic nature of the process under study. On the other hand, if two curves do not intercept

Table 7. Estimated (Centred and Scaled) Parameters Gathered Using the Global Optimization of the Objective Function (Global Minimum) and Refined Values (Final Estimate) Both in the Case of Numerical Experiments (Scheme 1) and Thermal Decomposition of Cumene Hydroperoxide

	Parameter Range		Numerical Experiments		Cumene Hydroperoxide	
Parameters	Lower Bound	Upper Bound	Global Minimum	Final Estimates	Global Minimum	Final Estimates
r	−8.00	−2.00	−4.56	−4.69	−4.34	−4.41
d	0.00	1.50	0.96	1.00	0.94	0.95
a	0.00	1.00	0.48	0.42	0.49	0.45
b	0.00	3.00	1.00	0.95	1.00	0.94

The second and third columns refer to the interval of parameters adopted when using glbsolve.

in a point different from the origin, RO(n) can describe the experimental data provided that $n > 0$ and SB(a,b) is not applicable. The identification of the kinetic model is performed by means of the introduction of suitable variables built by considering the data that come from two different experiments performed at different heating rate. A third run is required both to validate the kinetic model and gather reliable information about Arrhenius parameters by means of the application of the Kissinger's method. Once estimated, the final values of the whole set of parameters was obtained using a multivariate least square procedure. The conditions reported for the Case 1 provide a suitable tool for the identification of the autocatalytic nature of a thermal decomposition process. The results collected considering the thermal decomposition of CHP suggest the validity of the approach. For this compound, the following values of the apparent Arrhenius parameters were assessed $A = 3.728\text{E+}08\ \text{s}^{-1}$ and $E = 91{,}220\ \text{J mol}^{-1}$. The autocatalytic nature of this process was confirmed provided that RO(n) is not applicable and being the Sestak Berggren model suitable to describe the experimental data with exponents equal to $a = 0.45$ and $b = 0.93$. The methods proposed can also be applied to kinetic models different from RO or SB and allow the determination of the kinetic parameters, which should correspond to the global minimum of the objective function.

Notations

Roman symbols

a = first exponent in the SB model
A = apparent pre-exponential factor, s^{-1}
A_i = pre-exponential factor, ith reaction in Scheme 1, rate dependent
b = second exponent in the SB model
c = third exponent in the SB model
C_j = concentration of the jth species (Scheme 1), mol $(\text{dm}^3)^{-1}$
CHP = cumene hydroperoxide (80 w/w % in Cumene)
d = parameter in Eq. 20
E = apparent activation energy, J mol^{-1}
E_i = activation energy, ith reaction in Scheme 1, J mol^{-1}
$f(\alpha)$ = kinetic model
$f'(\alpha)$ = derivative of f
H = Hessian matrix
JMA(v) = Johnson–Mehl–Avramy model
$k_i(T)$ = kinetic constant, ith reaction in Scheme 1, rate expression depending
$K(T)$ = apparent kinetic constant, s^{-1}
m = temperature exponent in Eq. 4
M = mass, g
n = exponent in the reaction order model
N_i = number of experimental data points in the series at heating rate β_i
$\text{N}(\mu, \sigma^2)$ = Normal distribution with mean μ and variance σ^2
q = specific heat power, W g^{-1}
$q\ (\beta_i,t_{i,j})$ = measured heat power at β_i and $t_{i,j}$, W g^{-1}
r = parameter in Eq. 20
$R(n)$ = reaction order model
$R = 8.314$ = gas constant, J mol^{-1} K^{-1}
SB(a,b) = Sestack–Bergrenn model with exponents a and b
t = time, s or min
$t_{i,j}$ = jth time in the ith series of data, s or min
T = temperature, K
T_{end} = final temperature of a peak, K
$T_{i,\max}$ = temperature at the maximum of the ith peak, K
T_{Iso} = isothermal temperature, K
T_{Ref} = reference temperature in Eq. 20, K
V = volume, dm^3
x = variable in Eq. 14
y = variable in Eq. 14

Greek letters

α = conversion degree
$\alpha_{i,\max}$ = conversion at the maximum of the ith peak
β_i = heat rate (ith run), K min^{-1}
ΔH_{R} = heat of reaction, J g^{-1}
ΔH_i = heat of reaction, ith reaction in Scheme 1, J mol^{-1}
ε = heat power noise, J g^{-1}
Γ = curve on the plane (T, q)
φ_i = heat effect ith step (Scheme 1), J mol^{-1}
λ = eigen value
v = parameter in Johnson–Mehl–Avramy model
μ = mean
σ^2 = variance
$\underline{\vartheta}$ = vector of parameters
ξ = curve on the plane (T,α)
Ψ = objective function (sum of squared errors)

Subscripts and other symbols

$\hat{}$ = on a symbol indicates estimated parameter
$_0$ = as subscript indicates initial value or estimation
$\cap$ = intersection between sets
$\forall$ = for each (universal quantifier)
$\exists$ = there exist (existential quantifier)
: or | = in a logic expression indicates such that

Literature Cited

1. Šimon P. Considerations on the single-step kinetics approximation. *J Therm Anal Calorim*. 2005;82:651–657.
2. Šimon P. The single-step approximation—attributes, strong and weak sides. *J Therm Anal Calorim*. 2007;88:709–715.
3. Burnham AK, Dinh LN. A comparison of isoconversional and model-fitting approaches to kinetic parameter estimation and application predictions. *J Therm Anal Calorim*. 2007;89:479–490.
4. Khawam A, Flanagan DR. Complementary use of model-free and modelistic methods in the analysis of solid-state kinetics. *J Phys Chem B*. 2005;109:10073–10080.
5. Šimon P. Isoconversional methods: fundamentals, meaning and application. *J Therm Anal Calorim*. 2004;76:123–132.
6. Sewry JD, Brown ME. Model-free kinetic analysis? *Thermochim Acta*. 2002;390:217–225.
7. Vyazovkin S, Wight CA. Model-free and model-fitting approaches to kinetic analysis of isothermal and non-isothermal data. *Thermochim Acta*. 1999;340–341:53–68.
8. Opfermann JR, Kaisersberger E, Flammersheim H. J. Model-free analysis of thermoanalytical data-advantages and limitations. *Thermochim Acta*. 2002;391:119–127.
9. Pratap A, Shanker Rao TL, Lad KN, Dhurandhar HD. Isoconversional vs. model fitting methods, a case study of crystallization kinetics of a Fe-based metallic glass. *J Therm Anal Calorim*. 2007; 89:399–405.
10. Militký JZ, Sestak J. Building and statistical interpretation of non-isothermal kinetic models. *Thermochim Acta*. 1992;203:31–42.
11. Sestàk J, Berggren G. Study of the kinetics of the mechanism of solid-state reactions at increasing temperatures. *Thermochim Acta*. 1971;3:l–12.
12. Munteanu G, Segal E. Sestak–Berggren function in temperature-programmed reduction. *J Therm Anal Calorim*. 2010;101:89–95.
13. Burnham AK. Application of the Šesták–Berggren equation to organic and inorganic materials of practical interest. *J Therm Anal Calorim*. 2000;60:895–908.
14. Gorbatchev VM. Some aspects of Šestak's generalized kinetic equation in thermal analysis. *J Therm Anal*. 1980;18:193–197.
15. Frurip DJ, Elwell T. Effective use of differential scanning calorimetry in reactive chemicals hazard evaluation. *Process Saf Progr*. 2007;26:51–58.
16. Màlek J, Criado JM. Empirical kinetic models in thermal analysis. *Thermochim Acta*. 1992;203:25–30.
17. Budrugeac P. Theory and practice in the thermoanalytical kinetics of complex processes: application for the isothermal and non-isothermal thermal degradation of HDPE. *Thermochim Acta*. 2010; 500:30–37.
18. Bou-Diab L, Fierz H. Autocatalytic decomposition reactions, hazards and detection, *J Hazard Mater*. 2002;93:137–146.
19. Koga N, Sestak J, Malek J. Distortion of the Arrhenius parameters by the inappropriate kinetic model function. *Thermochim Acta*. 1991;188:333–336.

20. Saha B, Karthik Reddy P, Ghoshal AK. Hybrid genetic algorithm to find the best model and the globally optimized overall kinetics parameters for thermal decomposition of plastics. *Chem Eng J*. 2008;138:20–29.
21. Marcilla A, García-Quesada JC, Femenia RR. Letter to editor. *Thermochim Acta*. 2006;445:92–96.
22. Sbirrazzuoli N, Vincent L, Vyazovkin S. Comparison of several computational procedures for evaluating the kinetics of thermally stimulated condensed phase reactions. *Chemometr Intell Lab Syst*. 2000;54:53–60.
23. Màlek J. The kinetic analysis of non-isothermal data. *Thermochim Acta*. 1992;200:257–269.
24. de Britto D, Campana-Filho SP. Kinetics of the thermal degradation of chitosan. *Thermochim Acta*. 2007;465:73–82.
25. Màlek J, Sestàk J, Rouquerol F, Rouquerol J, Criado JM, Ortega A. Possibilities of two non-isothermal procedures (temperature- or rate-controlled) for kinetical studies. *J Therm Anal Calorim*. 1992; 38:71–87.
26. Malek J, Sestak J, Militky J. The boundary conditions for kinetic models. *Thermochim Acta*. 1989;153:429–432.
27. Llòpiz J, Romero MM, Jerez A, Laureiro Y. Generalization of the Kissinger equation for several kinetic models. *Thermochim Acta*. 1995;256:205–211.
28. Dun C, Xiang G, Dollimore D. A generalized form of the Kissinger equation. *Thermochim Acta*. 1993;215:109–117.
29. Matlab, software for scientific computing, online manuals and additional material. Available at http://www.mathworks.com/, accessed 2011.
30. Caballero JA, Conesa JA. Mathematical considerations for non-isothermal kinetics in thermal decomposition. *J Anal Appl Pyrol*. 2005;73:85–100.
31. Opfermann J. Kinetic analysis using multivariate non-linear regression. I. Basic concepts. *J Therm Anal Calorim*. 2000;60:641–658.
32. Varhegyi G, Szabo P, Jakab E, Till F. Least squares criteria for the kinetic evaluation of thermoanalytical experiments. Examples from a Char Reactivity Study. *J Anal Appl Pyrol*. 2001;57:203–222.
33. Rodionova OE, Pomerantsev AL. Estimating the parameters of the Arrhenius equation. *Kinet Catal*. 2005;46:305–308.
34. Buzzi-Ferraris G. Planning of experiments and kinetic analysis. *Catal Today*. 1999;52:125–132.
35. Watts DG. Estimating parameters in nonlinear rate equations. *Can J Chem Eng*. 1994;72:701–710.
36. Miyake A, Nomura K, Mizuta Y, Sumino M. Thermal decomposition analysis of organic peroxides using model-free simulation. *J Therm Anal Calorim*. 2008;92:407–411.
37. Miyake A, O'hama Y. Thermal hazard analysis of cumene hydroperoxide using calorimetry and spectroscopy. *J Therm Anal Calorim*. 2008;93:53–57.
38. Di Somma I, Andreozzi R, Canterino M, Caprio V, Sanchirico R. Thermal decomposition of cumene hydroperoxide: chemical and kinetic characterization. *AIChE J*. 2008;54:1579–1584.
39. Duh Y, Kao C, Lee C, Yu S. Runaway hazard assessment of cumene hydroperoxide from cumene oxidation process. *Process Saf Environ*. 1997;75:73–80.
40. Hattori K, Tanaka Y, Suzuki H, Ikawa T, Kubota H. Kinetic of liquid phase oxidation of cumene in bubble column. *J Chem Eng Jpn*. 1970;3:72–78.
41. Hou H, Shu C, Duh Y. Exothermic decomposition of cumene hydroperoxide at low temperature conditions. *AIChE J*. 2001;47:1893–1896.
42. Roduit B, Borgeat C, Berger B, Folly P, Alonso B, Aebischer JN, Stoessel F. Advanced kinetic tools for the evaluation of decomposition reactions—determination of thermal stability of energetic materials. *J Therm Anal Calorim*. 2005;80:229–236.
43. TOMLAB, optimization platform. Available at http://tomopt.com/tomlab/products/base/solvers/glbSolve.php, accessed 2011.
44. Björkman M, Holmström K. Global optimization using the DIRECT algorithm in Matlab. *Adv Model Optim*. 1999;1:17–37.
45. Jones DR, Perttunen CD, Stuckman BE. Lipschitzian optimization without the Lipschitz constant. *J Optim Theory Appl*. 1993;79: 157–181.

Manuscript received Mar. 4, 2011, and revision received May 30, 2011.